Cancer Gene Therapy (2022) 29:292–303
https://doi.org/10.1038/s41417-021-00309-5

ARTICLE

The LncRNA RP11-301G19.1/miR-582-5p/HMGB2 axis modulates the proliferation and apoptosis of multiple myeloma cancer cells via the PI3K/AKT signalling pathway

Faming Wang[1] · Yao Luo[1] · Le Zhang[1] · Muhammad Younis[2] · Liudi Yuan[1,2]

Received: 6 November 2020 / Revised: 26 January 2021 / Accepted: 5 February 2021 / Published online: 11 March 2021

Abstract

Long non-coding RNAs (lncRNAs) have recently been reported to act as crucial regulators and prognostic biomarkers of human tumorigenesis. Based on microarray data, RP11-301G19.1 was previously identified as an upregulated lncRNA during B cell development. However, the effect of RP11-301G19.1 on multiple myeloma (MM) cells remains unclear. In the present study, the effects of RP11-301G19.1 on tumour progression were ascertained both in vitro and in vivo. Our results demonstrated that RP11-301G19.1 was upregulated in MM cell lines and that its downregulation inhibited the proliferation and cell cycle progression and promoted the apoptosis of MM cells. Bioinformatic analysis and luciferase reporter assay results revealed that RP11-301G19.1 can upregulate the miR-582-5p-targeted gene HMGB2 as a competing endogenous RNA (ceRNA). Furthermore, Western blot results indicated that RP11-301G19.1 knockdown decreased the levels of PI3K and AKT phosphorylation without affecting their total protein levels. Additionally, in a xenograft model of human MM, RP11-301G19.1 knockdown significantly inhibited tumour growth by downregulating HMGB2. Overall, our data demonstrated that RP11-301G19.1 is involved in MM cell proliferation by sponging miR-582-5p and may serve as a therapeutic target for MM.

Introduction

Multiple myeloma (MM) accounts for more than 10% of haematologic malignancies and 1% of all cancers [1]. Furthermore, MM is capable of causing end-organ damage, including anaemia, hypercalcemia, renal insufficiency and osteolytic bone disease [2]. In recent decades, the number of patients with MM has continuously increased worldwide. Patients with MM have a short survival time, with a 40% 5-year survival rate. The aetiologies and potential molecular mechanisms of MM remain unclear [3]. Although great advancements have led to the development of numerous methods for the diagnosis and treatment of MM (e.g., immunomodulatory medicine, proteasome inhibitors and autologous stem cell transplantation), MM remains incurable [4, 5]. Therefore, the molecular mechanism underlying MM should be elucidated, and the development of feasible molecular targets is needed to treat patients with MM.

Long non-coding RNAs (lncRNAs) refer to a class of RNAs that are >200 nucleotides in length, have no protein-coding ability and lack complete open-reading frames [6]. The dysregulated expression of lncRNAs has been reported to contribute to the development of cancers (e.g., cancer metastasis, invasion and apoptosis) [7, 8], with several lncRNAs having been shown to be crucial in MM progression. For example, the lncRNA NEAT1 sponges miR-214 to regulate M2 macrophage polarization by regulating B7-H3 in MM [9]. In addition, LINC01234 promotes MM progression by regulating the miR-124-3p/GRB2 axis [10], while the long non-coding RNA CRNDE regulates the growth of MM cells through IL6 signalling [11]. MicroRNAs (miRNAs) constitute a

Supplementary information The online version contains supplementary material available at https://doi.org/10.1038/s41417-021-00309-5.

✉ Liudi Yuan
230179649@seu.edu.cn

[1] Department of Biochemistry and Molecular Biology, Medical School of Southeast University, Nanjing, China

[2] Key Laboratory for Developmental Genes and Human Disease, Ministry of Education, Institute of Life Sciences, Southeast University, Nanjing, China

group of endogenous, non-coding RNA (20–22 nt) [12]. The primary function of miRNAs is to bind the 3′UTRs of target genes and downregulate their expression [13]. Increasing evidence has shown that lncRNAs can act as ceRNAs to sponge miRNA and thus affect target gene expression. Shen et al. demonstrated that PCAT-1 promotes cell growth by sponging miR-129 via the MAP3K7/NF-κB pathway in MM [14]. Yang et al. demonstrated that lncRNA OIP5-AS1 loss-induced microRNA-410 accumulation regulates cell proliferation and apoptosis by targeting KLF10 via PTEN/PI3K/AKT pathway activation in MM [15]. LncRNAs and miRNAs have key roles in MM, but the underlying mechanisms remain to be elucidated.

The long non-coding RNA RP11-301G19.1 (ENST 00000412872) is a novel lncRNA that has gained increasing attention because of its crucial role in B cell development [16]. Nevertheless, the biological functions and underlying mechanisms of RP11-301G19.1, particularly in MM, remain largely unknown. MiR-582-5p has been demonstrated to have crucial roles in many tumours, with miR-582-5p upregulation having been shown to inhibit cell proliferation, cell cycle progression and invasion in human colorectal carcinoma [17]. In addition, miR-582-5p has been shown to suppress gastric cancer cell proliferation by targeting AKT3 [18]. Although the functions of miR-582-5p in some cancers have been demonstrated, its role in MM remains unclear.

High mobility group box 2 (HMGB2) was shown to be overexpressed in many cancers (glioblastoma, colorectal cancer, and hepatic carcinoma) and to function as an oncogene [19, 20]. For instance, HMGB2 can regulate hepatocellular carcinoma progression under the regulation of lncRNA PART1 and miR-590-3p [21]. In addition, HMGB2 can bind to and improve the activities of a number of transcription factors (such as p53, and p73) [22]. However, potential miRNAs targeting HMGB2 and its function in MM progression remain unclear.

In the present study, novel candidate lncRNAs were screened based on an analysis of published human immune-associated lncRNA datasets [16]. Subsequently, we examined the level of RP11-301G19.1 expression in MM cell lines. RP11-301G19.1 knockdown significantly inhibited cell proliferation and promoted cell apoptosis in MM. Mechanistically, we showed that RP11-301G19.1 may function as a molecular sponge for miR-582-5p to regulate the expression of HGMB2. In addition, we also observed that the PI3K/AKT pathway was regulated by RP11-301G19.1. Taken together, these results suggest that RP11-301G19.1 functions as an oncogene and may serve as a potential therapeutic target for the treatment of patients with MM.

Materials and methods

Cell culture and transfection

MM cell lines U266, RPMI8226, OPM-2, MM-1S, NCI-H929, normal plasma cells (nPCs) and 293T were purchased from the American Type Culture Collection (Manassas, VA, USA). MM cells and 293T cells were cultured in RPMI-1640 or DMEM medium (Thermo Fisher Scientific) supplemented with 10% heat-inactivated foetal bovine serum (FBS; Thermo Fisher Scientific), penicillin (100 U/ml) and streptomycin (100 U/ml) (Biosharp, Hefei, China) at 37 °C in a humidified atmosphere with 5% CO_2 incubator (Thermo Fisher Scientific). Short-hairpin RNA (shRNA) targeting RP11-301G19.1 (sh-RP11-301G19.1: 5′-AACACCGAACGAGACACGATT-3′) along with corresponding non-targeting sequences (sh-NC: 5′-TGTTCGACCTTTCCCAAATTA-3′) was synthesized and inserted into the PLKO.1 plasmid (Gene-Pharma, Shanghai, China). 293T cells were used to transfect and harvest lentiviruses. U266 and RPMI8226 were infected with the obtained lentivirus. puromycin (5 mg/mL; Sigma-Aldrich) was used for selection of stably infected cells. miR-582-5p mimics (miR-582-5p mimic), miR-582-5p inhibitors (miR-582-5p inh) and their corresponding controls (NC-mimic or NC inh) were purchased from Genechem (Shanghai, China). The sequence of HMBG2 was cloned into pCDNA (Invitrogen) to construct the overexpression vector pCDNA-HMGB2 with pCDNA as the negative control. All transfections were conducted using Lipofectamine 2000 (Invitrogen). The efficiency of transfection was assessed by real-time quantitative real-time polymerase chain reaction (qRT-PCR) 48 h after transfection.

qRT-PCR analysis

Total RNA were extracted from the cultured cells using TRIzol® reagent (Thermo Fisher Scientific). CDNA was synthesized from total RNA using the HiScript II 1st Strand cDNA Synthesis Kit (Vazyme Biotech, Nanjing, China). SYBR Premix Ex Taq (Takara, Shiga, Japan) was used to perform qRT-PCR assays. A SYBR PrimeScript miRNA RT-PCR Kit (Takara) was used to examine miRNA levels. The relative expression of target genes was calculated using the $2^{-\Delta\Delta CT}$ method. Primers were as following: RP11-301G19.1: forward, 5′-ACCTATTTCTACCCACAATCCACC-3′ and reverse, 5′-ACCTGAACCCGAACTATTCCTTT-3′; miR-582-5p: forward, 5′-ATCCCTAGCTTCAACGTG-3′ and reverse, 5′-CGTTACAATTGCTAGC-3′; HMGB2: forward, 5′-GGGGAAGAAAAAGGACCCCA-3′ and reverse, 5′-GC TGACTGCTCAGACCACAT-3′; GAPDH: forward, 5′-ACA ACTTTGGTATCGTGGAAGG-3′ and reverse, 5′-GCCAT CACGCCACAGTTTC-3′; XIST: forward, 5′-TCATCGGA GGGCTAAAGTGG-3′ and reverse, 5′-CAACAGCTGCCA ATAAAAG-3′.

Subcellular fractionation

The part of nuclear and cytoplasm were extracted from the cultured cells using the PARIS Kit (Sigma). Then, the qRT-PCR was performed to explore the expression level of RP11-301G19.1, GAPDH and XIST in cytoplasm or nuclear of the cells. XIST and GAPDH were served as positive controls.

Cell proliferation assay

Cell proliferation was explored using cell counting kit-8 (CCK-8; Biosharp), according to the manufacturer's protocol. MM cells were seeded into 96-well culture plates at a density of 2×10^3 cells/well in 100 µl medium. Cell growth rate was assessed every 24 h according to the manufacturer's instructions. 10 µl of CCK-8 was added to each well and incubated at 37 °C for 2 h. After that, the optical density of each well was measured using Envision (Perkin Elmer Biotech Co., Ltd.) at 450 nm.

Colony formation assay

U266 or RPMI8226 cells (1×10^3) were mixed into top agar (1.5 ml), and then added onto base agar. 3 weeks later, colonies were stained by Crystal Violet. And a dissection microscope (TE2000-U, Nikon, Japan) was used to count the colonies.

Cell cycle and cell apoptosis assay

Cells were fixed in 70% ice-cold ethanol (Wanqing, Nanjing, China) for 2 h and incubated with propidium iodide (PI, Vazyme). Annexin V-FITC apoptosis detection kit (Vazyme) was used for cell apoptosis assay. Then, a FACS Calibur system (BD Biosciences, San Jose, CA) was used for DNA content and Annexin V analysis. The results of cell cycle and cell apoptosis were analysed using the ModFit_LT software

Luciferase reporter assay

The lncRNASNP2 (http://bioinfo.life.hust.edu.cn/lncRNASNP) and LncBase V.2 (http://carolina.imis.athena-innovation.gr/diana_tools/web/index) databases were used to predict miRNAs that target RP11-301G19.1. Target genes of miRNAs were analysed using TargetScan, StarBase and miRDB. An RP11-301G19.1 fragment with the predicted binding sites for miR-582-5p and the 3′UTR of HMGB2 (with binding sites for miR-582-5p) was inserted into the pGL3-Control vector to generate the luciferase reporter plasmids RP11-301G19.1-WT and HMGB2-WT. Mutant luciferase vectors (RP11-301G19.1-MUT and HMGB2-MUT) were constructed using a site-directed mutagenesis kit. The luciferase reporter plasmids and miR-582-5p mimics or NC mimics were cotransfected into 293T cells using Lipofectamine 2000. After 48 h of transfection, the relative luciferase activities were measured using a dual-luciferase reporter assay system according to the manufacturer's instructions.

Western blot analysis

Cells were lysated using RIPA lysis buffer (Biosharp) containing protease inhibitor PMSF. The protein concentration was measured using the BCA Protein assay kit (Biosharp). The membranes incubated with corresponding primary antibody, cyclin D1 (Proteintech, 1:500), Rb (Proteintech, 1:500), P16 (Proteintech, 1:1000), Bcl-2 (Proteintech, 1:2000), Bax (Proteintech, 1:3000), Caspase-3 (Proteintech, 1:800), HMGB2 (Proteintech, 1:1000), p-PI3K (CST, 1:1000), t-PI3K (CST, 1:1000), t-AKT (Abcam, 1:1000), p-AKT (Abcam, 1:500) and GAPDH (Proteintech, 1:10,000) at 4 °C overnight, and incubated with anti-mouse/anti-rabbit IgG (Abbkine, 1:3000) at room temperature for 1 h. Protein bands were quantified using Gel-Pro Analyzer (Media Cybernetics, Rockville, MD, USA).

Xenograft tumour mouse models

RPMI8226 cells (2×10^6) stably transfected with sh-RP11-301G19.1 or sh-NC were implanted into the right and left backside regions of female BALB/c-nude mice (18–20 g) that were obtained from the Comparative Medicine Center of Yangzhou University ($n = 10$/group). The tumour volume (V) was monitored by measuring the length (L) and width (W) of tumours every 3 days with callipers and was calculated using the following formula: volume = (length × width^2)/2. Thirty days after tumour cell inoculation, the mice were sacrificed, and the xenograft tumours were resected, measured and imaged. The animal study was approved by the Ethics Committee of Southeast University (20200701007, 01 July 2020). All animal experiments were performed in accordance with the Guide for the Care and Use of Laboratory Animals of the National Institutes of Health [23].

Statistical analysis

All experiments were performed at least three times. The data were statistically analysed by using either SPSS 23.0 (SPSS, Chicago, IL, USA) or GraphPad Prism 7.0 software (GraphPad Software, La Jolla, CA, USA). All quantitative results are presented as the mean ± standard deviation (SD). Student's t-test was used to analyse the differences between two groups. One-way ANOVA was used to analyse the

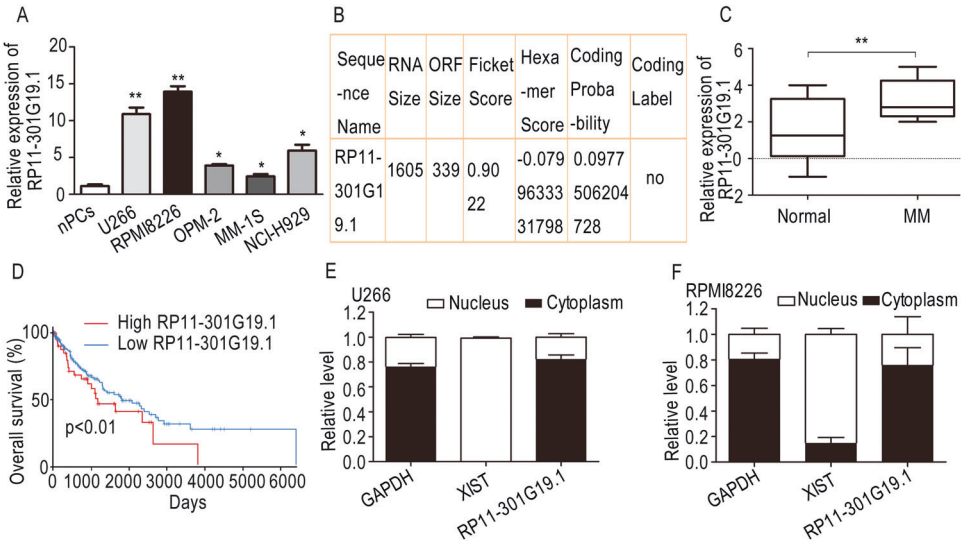

Fig. 1 RP11-301G19.1 is upregulated in human MM tissues and cell lines. A The relative level of RP11-301G19.1 expression was significantly higher in MM cell lines than in normal plasma cells (nPCs) (one-way ANOVA). **B** Coding potential assessment tool (CPAT) was used to calculate the coding capability of RP11-301G19.1. **C** The relative expression of RP11-279C4.1 in MM and normal tissues was analysed using the GSE24080 public database (Student's *t*-test). **D** The association of RP11-279C4.1 expression in MM and overall patient survival rate was analysed using the GSE24080 public database. **E**, **F** Fractionation of U266 and RPMI8226 cells followed by qRT-PCR was performed to assess the localization of RP11-301G19.1. GAPDH served as the control for cytoplasmic expression, and XIST was the control for nuclear expression (Student's *t*-test). The data is presented as mean ± SD (standard deviation) from three independent experiments. $*P < 0.05$, $**P < 0.01$.

differences among multiple groups. $P < 0.05$ was considered to indicate a significant difference. $*P < 0.05$; $**P < 0.01$; $***P < 0.001$.

Results

RP11-301G19.1 is upregulated in human MM tissues and cell lines

The levels of RP11-301G19.1 in the MM cells and nPCs were assessed by qRT-PCR. RP11-301G19.1 expression was significantly higher in the MM cells than in the nPCs (Fig. 1A). To confirm the non-coding potential of RP11-301G19.1, the present study blasted the sequences of RP11-301G19.1 by using online software Coding Potential Assessment Tool (CPAT v2.0.0) [24]. The value for RP11-301G19.1 obtained from the CPAT database indicates that RP11-301G19.1 is a non-coding RNA (Fig. 1B). Importantly, we also assessed RP11-301G19.1 expression levels in MM tissues by analysing data from a public dataset of patients profiled (GSE24080, Affymetrix HG-U133_Plus_2.0 array). The results indicated that compared to that observed in normal tissues, RP11-301G19.1 expression was significantly elevated in MM tissues (Fig. 1C). Similarly, Kaplan–Meier survival analysis using the GSE24080 public database suggested that the overall survival rate of MM patients with low RP11-279C4.1 expression is higher (Fig. 1D). Additionally, we observed that RP11-301G19.1 was primarily localized in the cytoplasm of U266 and RPMI8226 cells (Fig. 1E, F). The above data indicated that RP11-301G19.1 may impact the genesis of MM.

RP11-301G19.1 downregulation inhibits MM cell proliferation

To ascertain the function of RP11-301G19.1, sh-RP11-301G19.1 lentivirus was used to knock down the endogenous expression of RP11-301G19.1 in MM cells (Fig. 2A). CCK-8 assays were performed to assess MM cell proliferation. As shown in Fig. 2, RP11-301G19.1 downregulation led to a significant decrease in the viability of U266 (Fig. 2B) and RPMI8226 (Fig. 2C) cells. To further confirm the effects of RP11-301G19.1 on cell proliferation, colony-formation assays were performed. The results suggested that RP11-301G19.1 downregulation significantly decreased the colony-forming ability of U266 and RPMI8226 cells (Fig. 2D).

RP11-301G19.1 affects the cycle progression and apoptosis of MM cells

We performed flow cytometry assays to assess the effect of RP11-301G19.1 on the cell cycle and apoptosis of MM cells. According to the FACS results, RP11-301G19.1 silencing led to a marked increase in the number of U266 and RPMI8226 cells in the G_1 phase cell

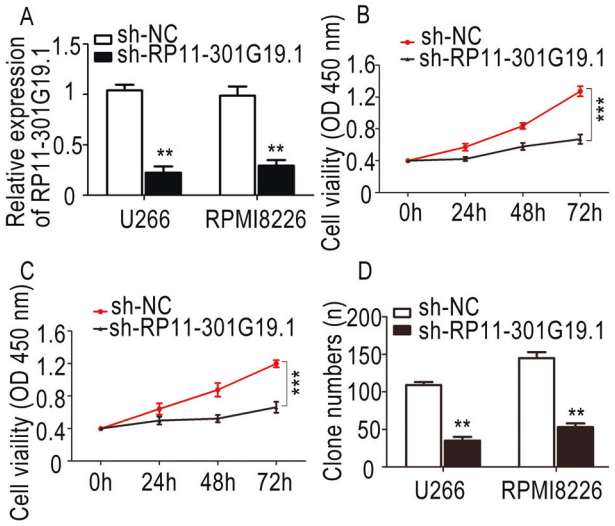

Fig. 2 RP11-301G19.1 enhances the proliferation of MM cells. A *RP11-301G19.1* knockdown with sh-RNA in U266 and RPMI8226 cell lines. GAPDH was used as an internal reference (Student's *t*-test). **B**, **C** Cell proliferation was measured using the CCK-8 assay of U266 and RPMI8226 cells at the indicated time points (24, 48 and 72 h) after they were seeded in a 96-well plate (Student's *t*-test). **D** A soft agar colony formation assay was conducted, and the quantification results are shown in histograms (Student's *t*-test). The data is presented as mean ± SD (standard deviation) from three independent experiments. $^{**}P < 0.01$, $^{***}P < 0.001$.

population and a decrease in number in the S-phase (Fig. 3A). Additionally, as shown in Fig. 3B, RP11-301G19.1 downregulation significantly increased the percentage of apoptotic cells. The Western blot analysis data showed that the levels of cell cycle-associated proteins (Cyclin D1, Rb and p16) and cell apoptosis-related proteins (Bcl-2, Bax and Caspase-3) were significantly altered after RP11-301G19.1 knockdown (Fig. 3C). The above results demonstrated that RP11-301G19.1 knockdown significantly inhibited the cell cycle progression and induced the apoptosis of U266 and RPMI8226 cells.

RP11-301G19.1 regulates the miR-582-5p/HMGB2 axis in MM

As indicated above, RP11-301G19.1 was observed to be primarily located in the cytoplasm. To investigate the mechanism by which RP11-301G19.1 affects MM cell proliferation, cell cycle progression and apoptosis, we predicted the potential target miRNAs using bioinformatics tools (lncRNASNP2 and LncBase V.2) and selected four miRNAs for further analysis (Fig. 4A). We assessed the expression of four miRNAs in MM cell lines and nPCs and observed that only miR-582-5p expression was significantly lower in the MM cell lines than it was in the nPCs (Fig. 4B). In addition, we conducted dual-luciferase reporter assay to evaluate these four miRNAs further.

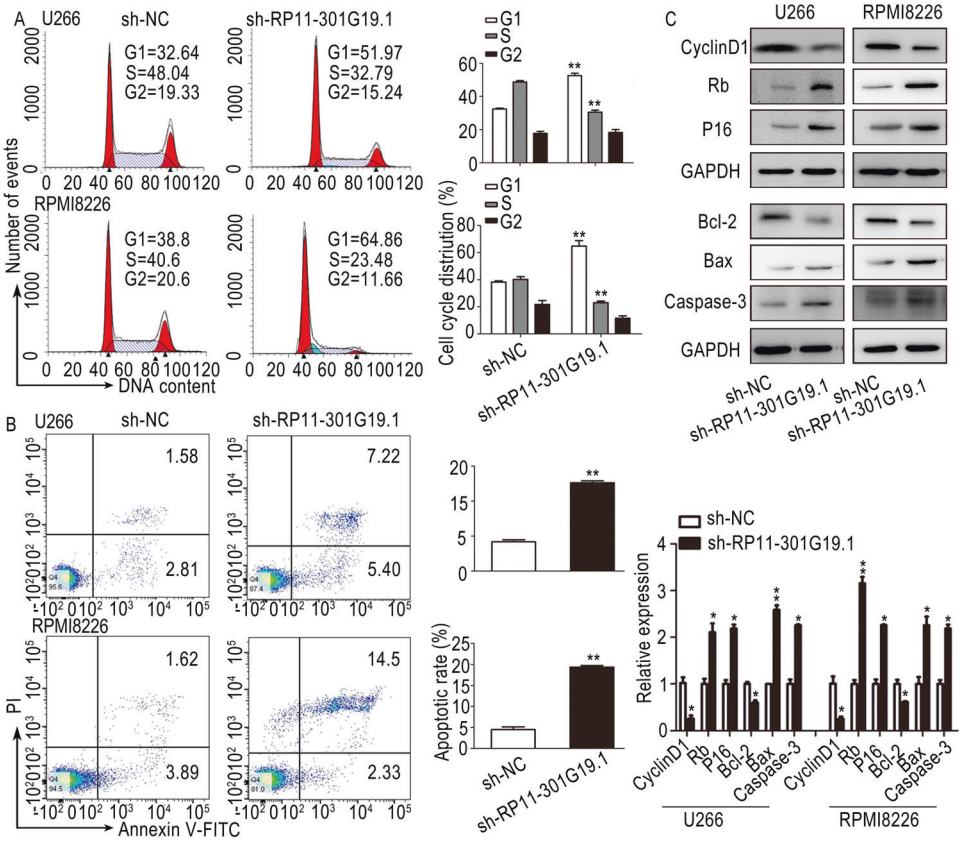

Fig. 3 RP11-301G19.1 affects the cycle progression and apoptosis of MM cells. A The cell cycle distribution of U266 and RPMI8226 cells with RP11-301G19.1 knockdown was determined by PI staining and FACS analysis. The histograms present the percentages of cells in G1, S, and G2 phases (Student's *t*-test). **B** RPMI8226 and U266 cell apoptosis was detected by flow cytometry after staining with PI/Annexin V-FITC. The percentages of apoptotic cells are presented in histograms (Student's *t*-test). **C** The protein levels of Cyclin D1, Rb, P16, Bcl-2, Bax and Caspase-3 in U266 and RPMI8226 cells with RP11-301G19.1 downregulation were measured by Western blotting. The relative quantitative results were determined using ImageJ and are shown in histograms (Student's *t*-test). The data is presented as mean ± SD (standard deviation) from three independent experiments. $^{*}P < 0.05$, $^{**}P < 0.01$.

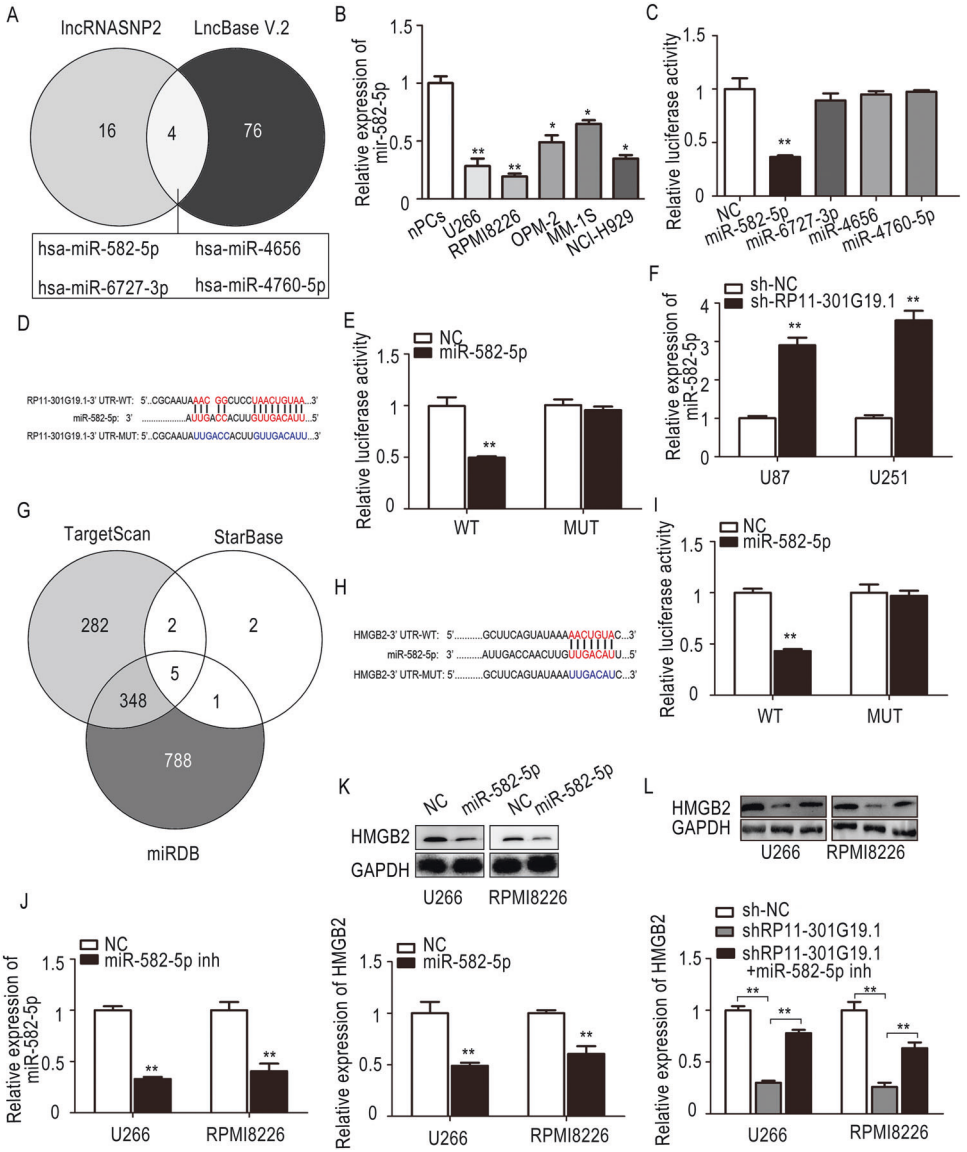

Fig. 4 RP11-301G19.1 regulates the miR-582-5p/HMGB2 axis in MM. A The LncBase V.2 and lncRNASNP2 databases were used to screen four miRNAs capable of binding RP11-301G19.1. **B** The level of miR-582-5p expression in MM cells compared to that in nPCs was examined by qRT-PCR (one-way ANOVA). **C** Luciferase activity was measured after cells were co-transfected with four various miRNA mimics and plasmids containing the RP11-301G19.1 sequence (Student's *t*-test). **D** The predicted direct binding site of RP11-301G19.1 and miR-582-5p. **E** The relative luciferase activity of the RP11-301G19.1 reporter plasmid (wild-type or mutant) was detected in 293T cells after they were transfected with miR-582-5p mimics or NC mimics (Student's *t*-test). **F** The relative miR-582-5p expression levels in RP11-301G19.1-knockdown cells were analysed by qRT-PCR (Student's *t*-test). **G** The TargetScan, miRDB and StarBase databases were used to identify the target genes of miR-582-5p. **H** The direct binding sites of HMGB2 and miR-582-5p. **I** The relative luciferase activity of the HMGB2 3'UTR reporter plasmid (wild-type or mutant) was detected in 293T cells after transfected with miR-582-5p mimics or NC mimics (Student's *t*-test). **J** The relative miR-582-5p expression levels in MM cells transfected with miR-582-5p inhibitors (miR-582-5p inh) was determined by qRT-PCR (Student's t-test). **K** Western blot analysis was performed to determine the protein levels of HMGB2 in MM cells transfected with miR-582-5p mimics or NC mimics (Student's *t*-test). **L** Western blot analysis was performed to determine the protein levels of HMGB2 in MM cells transfected with sh-NC, sh-RP11-301G19.1 and sh-RP11-301G19.1+miR-582-5p inh. The relative quantitative results were determined using ImageJ and are shown in histograms (one-way ANOVA). The data is presented as mean ± SD (standard deviation) from three independent experiments. $^{*}P < 0.05$, $^{**}P < 0.01$.

The results showed that luciferase activity was markedly suppressed by miR-582-3p (Fig. 4C). To confirm the direct binding between RP11-301G19.1 and miR-582-5p, we constructed reporter plasmids (RP11-301G19.1-WT or RP11-301G19.1-MUT) and cotransfected them into cells with miR-582-5p mimics or NC mimics (Fig. 4D). The results revealed that miR-582-5p mimics significantly decreased the luciferase activity of RP11-301G19.1-WT, while this suppression was not observed in the presence of RP11-301G19.1-MUT (Fig. 4E). Moreover, we observed that RP11-301G19.1

knockdown significantly increased miR-582-5p expression (Fig. 4F). However, the function of miR-582-5p in MM remained unclear. Therefore, we subsequently used TargetScan, miRDB and StarBase to predict target genes for miR-582-5p (Fig. 4G). The results identified HMGB2 as the best candidate target gene of miR-582-5p. Accordingly, we constructed luciferase reporter constructs to verify whether HMGB2 expression is regulated by miR-582-5p (Fig. 4H). As shown in Fig. 4I, miR-582-5p upregulation decreased the luciferase activity of HMGB2-WT group, while no difference was observed in the HMGB2-MUT group. qRT-PCR was performed to assess the level of miR-582-5p expression, and the results demonstrated that miR-582-5p levels were decreased after treatment with miR-582-5p inhibitors (miR-582-5p inh) (Fig. 4J). Additionally, after the cells were transfected with miR-582-5p mimics, HMGB2 protein levels were markedly decreased (Fig. 4K). Moreover, HMGB2 protein levels were remarkably decreased after RP11-301G19.1 knockdown. However, the miR-582-5p inhibitors reversed this reduction (Fig. 4L). These results suggested that RP11-301G19.1 may regulate HMGB2 expression by sponging miR-582-5p.

RP11-301G19.1 affects MM cell proliferation, cell cycle progression and apoptosis by regulating miR-582-5p expression

Subsequently, we performed rescue experiments to assess whether RP11-301G19.1 exerts biological functions in MM through miR-582-5p. CCK-8 assay results revealed that RP11-301G19.1 downregulation significantly inhibited cell growth, and this reduction was restored by simultaneously inhibiting RP11-301G19.1 and miR-582-5p (Fig. 5A, B). The results presented in Fig. 5C indicated that RP11-301G19.1 knockdown efficiently decreased colony numbers, and this suppression could be restored by simultaneously inhibiting RP11-301G19.1 and miR-582-5p. Additionally, the FACS results indicated that sh-RP11-301G19.1 treatment resulted in cell cycle arrest at G0/G1 phase, an effect that was abolished by co-transfecting cells with sh-RP11-301G19.1 and miR-582-5p inhibitors (Fig. 5D). In addition, as shown in Fig. 5E, the apoptotic rate of cells was significantly upregulated after RP11-301G19.1 downregulation in U266 and RPMI8226, whereas after simultaneously inhibiting RP11-301G19.1 and miR-582-5p, the apoptotic rate was significantly decreased. These results demonstrated that RP11-301G19.1 downregulation significantly suppressed U266 and RPMI8226 cell proliferation and cell cycle progression and promoted their apoptosis by depending on the negative regulation of miR-582-5p.

PI3K/AKT signalling plays an important role in the RP11-301G19.1-mediated biological process of MM cells

To assess whether PI3K/AKT signalling is involved in the RP11-301G19.1/miR-582-5p/HMGB2 axis mediated biological process of MM cells, we first constructed and transfected cells with the vector pCDNA-HMGB2 and observed that HMGB2 expression was markedly increased (Fig. 6A, B). We further identified the underlying effects of HMGB2 on MM cell proliferation. CCK8 cell proliferation was preformed to detect the cell growth abilities after HMGB2 oevrexpression. The results showed that the cell proliferation abilities were ehanced after HMGB2 overexpressing in U266 and RPMI8226 cells (Supplementary Fig. 1). Then, we evaluated the levels of t-PI3K, p-PI3K, t-AKT and p-AKT. The results revealed that RP11-301G19.1 downregulation significantly inhibited the protein levels of p-PI3K and p-AKT, and this inhibition was restored by co-transfecting cells with sh-RP11-301G19.1 and pCDNA-HMGB2. In contrast, the total protein (t-PI3K and t-AKT) levels did not change in U266 cells (Fig. 6C). Furthermore, we also obtained similar results with RPMI8226 cells (Fig. 6D). These results demonstrated that PI3K/AKT signalling plays an essential role in the RP11-301G19.1/miR-582-5p/HMGB2 axis-mediated biological process of MM cells.

RP11-301G19.1 downregulation inhibits MM cell tumorigenesis in vivo

We further assessed the function of RP11-301G19.1 in vivo using xenograft tumour mouse models. RPMI8226 cells transfected with sh-RP11-301G19.1 or sh-NC) were subcutaneously implanted into two groups of nude mice. After 6 days, all mice developed detectable tumours. The representative image of the tumours shown in Fig. 7A shows that the sizes of the tumours were significantly different between the two groups. In addition, the tumours in the sh-RP11-301G19.1 group also weighed less compared to those from the sh-NC group (Fig. 7B). Furthermore, RP11-301G19.1 levels were significantly decreased in xenograft tumours (Fig. 7C), which led to higher of miR-582-5p expression (Fig. 7D). In addition, HMGB2 expression in xenograft tumours was monitored via Western blot analysis, the results of which showed that RP11-301G19.1 knockdown evidently lowered the level of HMGB2 expression (Fig. 7E). These results indicated that RP11-301G19.1 downregulation could increase miR-582-5p expression, suppress the protein expression of HMGB2, decrease cell proliferation and inhibit MM cell growth in vivo.

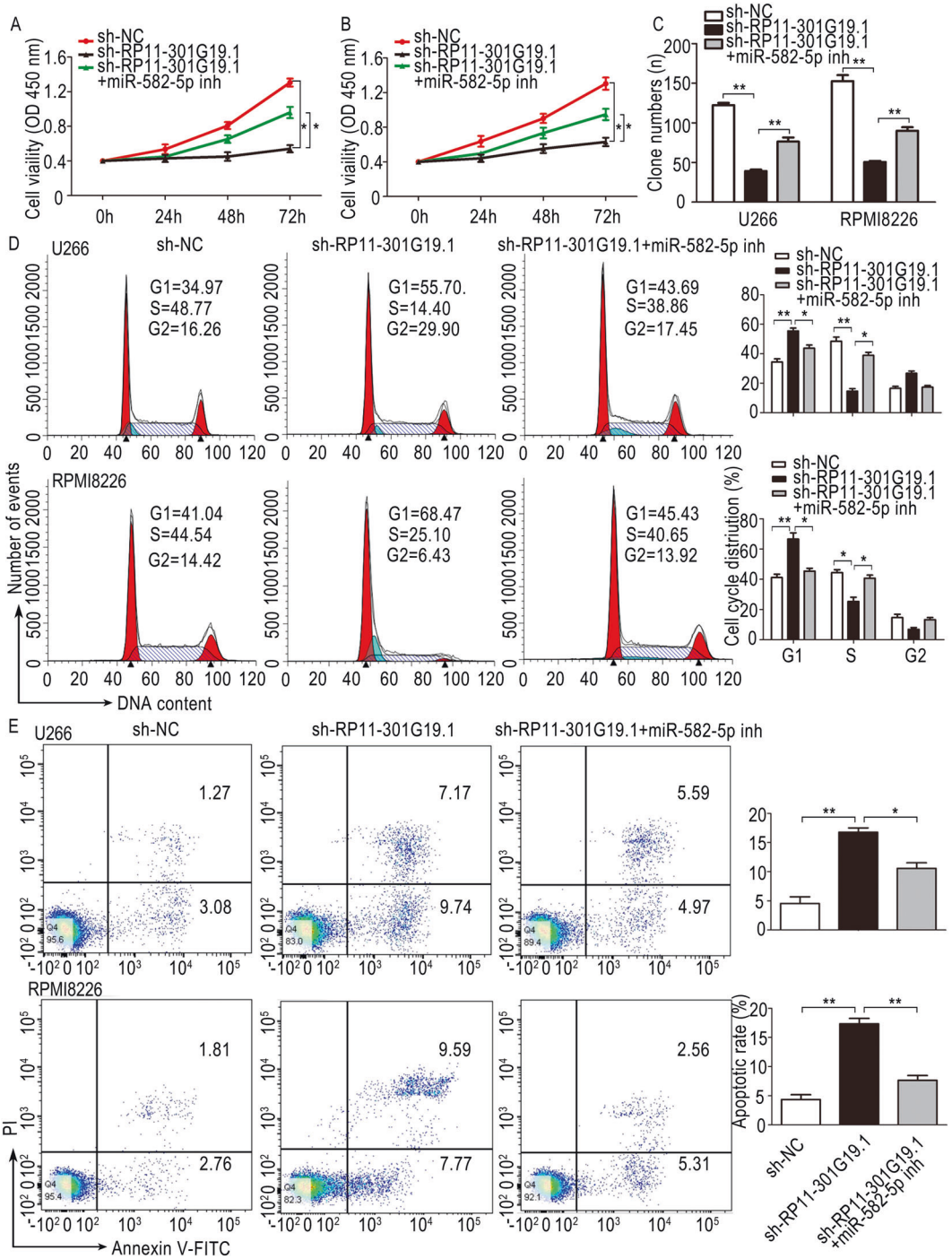

Fig. 5 RP11-301G19.1/miR-582-5p signalling affects the proliferation, cell cycle progression and apoptosis of MM cells. A, **B** Cell counting kit-8 (CCK-8) assay was used to measure the proliferation of MM cells transfected with sh-NC, sh-RP11-301G19.1 and sh-RP11-301G19.1+miR-582-5p inh (one-way ANOVA). **C** The colony formation numbers for MM cells transfected with sh-NC, sh-RP11-301G19.1 and sh-RP11-301G19.1+miR-582-5p inh are shown in histograms (one-way ANOVA). **D** The cell cycle distribution of MM cells transfected with sh-NC, sh-RP11-301G19.1 and sh-RP11-301G19.1+miR-582-5p inh were determined by PI staining and FACS analysis. The histograms show the percentages of cells in the G1, S, and G2 phases (one-way ANOVA). **E** The apoptosis rate of MM cells transfected with sh-NC, sh-RP11-301G19.1 and sh-RP11-301G19.1 +miR-582-5p inh was detected by flow cytometry after the cells were stained with PI/Annexin V-FITC (one-way ANOVA). The percentages of apoptotic cells are presented in histograms. The data is presented as mean ± SD (standard deviation) from three independent experiments. $*P < 0.05$, $**P < 0.01$.

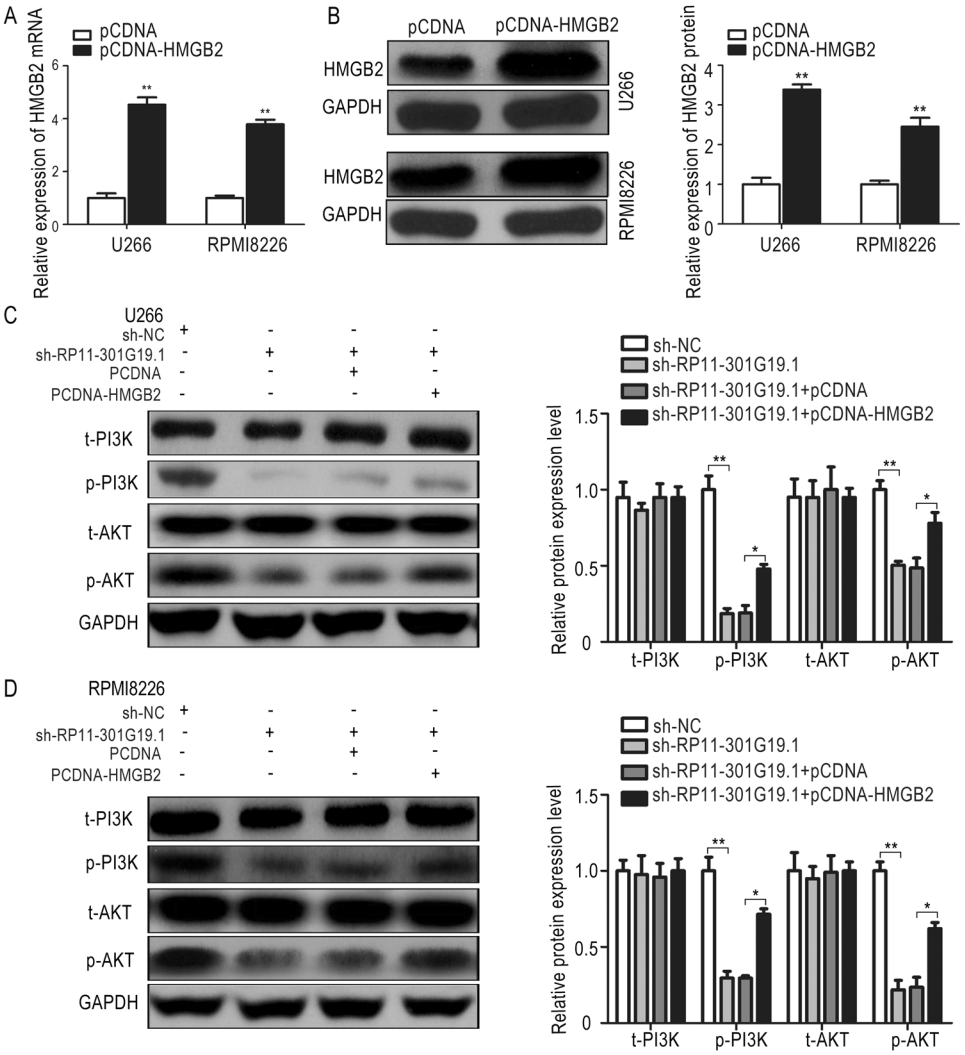

Fig. 6 HMGB2 restores the RP11-301G19.1-mediated inhibition of PI3K/AKT signalling in MM cells. A The mRNA levels of HMGB2 in the MM cells transfected with pCDNA-HMGB2 were examined by qRT-PCR (Student's *t*-test). **B** The protein levels of HMGB2 in the MM cells transfected with pCDNA-HMGB2 were examined by Western blotting (Student's *t*-test). **C**, **D** Western blot analysis of t-PI3K, p-PI3K, t-AKT and p-AKT protein levels in MM cells transfected with sh-NC, sh-RP11-301G19.1, sh-RP11-301G19.1+pCDNA and sh-RP11-301G19.1+pCDNA-HMGB2. Relative quantitative results were determined using ImageJ and are shown as histograms (Student's *t*-test). The data is presented as mean ± SD (standard deviation) from three independent experiments. $^{*}P < 0.05$, $^{**}P < 0.01$.

Discussion

MM refers to a neoplasm of terminally differentiated B cells (plasma cells) in which chromosome translocations frequently lead to oncogene formation under the regulation of immunoglobulin enhancers [25]. Increasing evidence has shown that the dysregulation of lncRNAs contributes to the genesis and progression of MM [26, 27]. For instance, lncRNA PVT1 is associated with the pathogenesis and progression of MM. In addition, PVT1 expression is associated with poor MM patient survival [28], and lncRNA OIP5-AS1 can repress MM progression in vitro and in vivo through modulation of the miR-27a-3p/TSC1 axis [29]. RP11-301G19.1 was evaluated in the present study, which is 1605 nucleotides in length, located on chromosome 6 (start: 68597538; end: 6859923;—stand), and comprises two exons. Our qRT-PCR data showed RP11-301G19.1 was highly expressed in MM cells and primarily localized in the cytoplasm. Moreover, RP11-301G19.1 knockdown led to a notable suppression of MM cell proliferation and clonogenicity and induced apoptosis. The results of in vivo analyses indicated that RP11-301G19.1 silencing could suppress tumour growth. Therefore, our data demonstrated, for the first time, that RP11-301G19.1 is a novel oncogene in MM.

The results of a growing number of studies have indicated that lncRNAs serve as molecular sponges in tumour cells. For instance, H19 was shown to inhibit the apoptosis of MM cells and promote BTZ resistance by regulating the translation of MCL-1 and silencing miR-29b-3p [30]. SNHG16 suppresses MM cell proliferation, induces cell cycle arrest, and promotes apoptosis by sponging miR-342-3p [31]. In our present study, we predicted that RP11-301G19.1 targets miR-582-5p through a bioinformatics analysis. The direct interaction of RP11-301G19.1 and miR-582-5p was confirmed through luciferase activity reporter assays. In addition, we also observed that RP11-301G19.1 knockdown increased miR-582-5p expression. MiR-582-5p has important roles in cancers and can regulate cell proliferation and apoptosis by targeting AKT3 in human endometrial carcinoma [32]. MiR-582-5p restrains

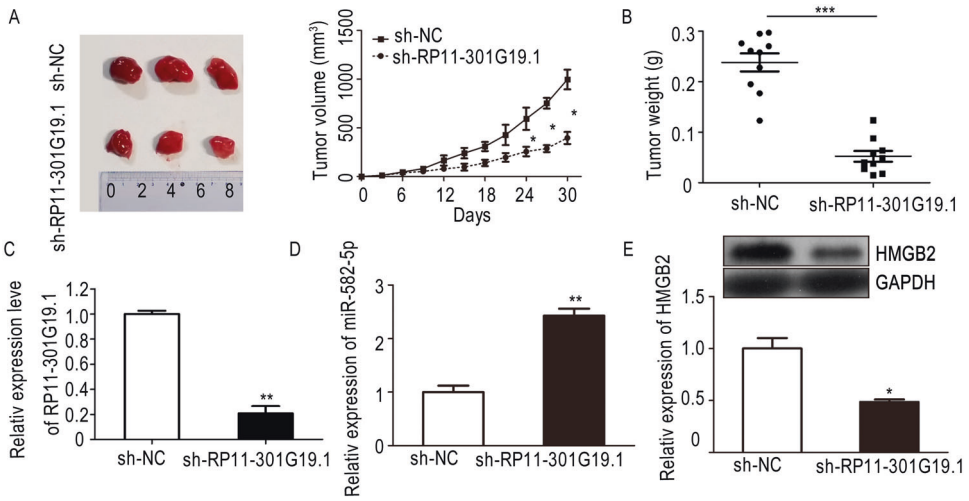

Fig. 7 RP11-301G19.1 downregulation inhibits MM cell tumorigenesis in vivo. A Macroscopic appearance of the xenograft tumours in nude mice injected with RPMI8226 cells ($n = 10$). Tumour volume was calculated every 3 days (Student's *t*-test). **B** The tumour weight of each tumour sample from the two groups are shown (Student's *t*-test). **C** The relative expression levels of RP11-301G19.1 in the xenograft tumours formed by the sh-NC-treated or sh-RP11-301G19.1-treated cells were determined by qRT-PCR (Student's *t*-test). **D** The relative expression levels of miR-582-5p in the xenograft tumours formed by the sh-NC-treated or sh-RP11-301G19.1-treated cells were determined by qRT-PCR (Student's *t*-test). **E** Western blot analysis was performed to determine the protein levels of HMGB2 in xenograft tumours formed by sh-NC-treated or sh-RP11-301G19.1-treated cells (Student's *t*-test). The data is presented as mean ± SD (standard deviation) from three independent experiments. $^{*}P < 0.05$, $^{**}P < 0.01$, $^{***}P < 0.001$.

cell growth and the invasive potential of NSCLC by downregulating NOTCH1 [33]. In addition, miR-582-5p can be used as an independent prognostic biomarker for patients with NSCLC [34]. However, the role of miR-582-5p in MM has remained unclear. Interestingly, the results of our present study suggest that miR-582-5p is a tumour suppressor in MM.

Therefore, the potential target genes of miR-582-5p were predicted using TargetScan, miRDB and StarBase, the results of which showed that miR-582-5p targets HMGB2 in MM. Previous studies reported that HMGB2 plays a role in the ability of the HOXA11-AS/miR-130a-5p axis to regulate the growth and metastasis of glioma [35]. HMGB2 can promote cancer cell growth and lead to poor patient prognosis by activating the AKT signalling pathway [36, 37]. In our present study, we observed that HMGB2 overexpression or miR-582-5p inhibition partially reversed the effects of RP11-301G19.1 knockdown on MM cell proliferation. Moreover, PI3K and AKT activation could be restored by overexpressing HMGB2 in the sh-RP11-301G19.1 group. This result demonstrated that RP11-301G19.1 inhibits cellular functions through the PI3K/AKT pathway in MM. A limitation of this work is that we did not assess the expression levels of this newly identified ceRNA triplet in MM clinical samples. In addition, the clinical significance of these genes in MM was not investigated.

In summary, the results of our present study identified a novel lncRNA, RP11-301G19.1, as a crucial mediator of cell proliferation and apoptosis in MM. Our findings demonstrated that RP11-301G19.1 was identified upregulated in MM cell lines. RP11-301G19.1 downregulation impaired tumour cell growth in vitro and in vivo. RP11-301G19.1 was shown to function as a sponge for miR-582-5p to affect HMGB2 expression. Thus, our results indicate that intervention of the RP11-301G19.1/miR-582-5p/HMGB2 regulatory pathway can inhibit MM progression through the PI3K/AKT pathway.

Data availability

All data generated or analysed during this study are included in this published article.

Funding This study was supported by the Graduate Research and Innovation Projects of Jiangsu Province (KYCX19_0114).

Compliance with ethical standards

Conflict of interest The authors declare no competing interests.

Publisher's note Springer Nature remains neutral with regard to jurisdictional claims in published maps and institutional affiliations.

References

1. Manasanch E, Munshi NC, Nooka AK, Rapoport AP, Smith EL, Vij R, et al. The Society for Immunotherapy of Cancer consensus statement on immunotherapy for the treatment of multiple

myeloma. J Immunother Cancer. 2020;8:e000734 https://doi.org/10.1136/jitc-2020-000734
2. Chiu E, Cabanero M, Sidhu G. Paradoxical stress fracture in a patient with multiple myeloma and bisphosphonate use. Cureus. 2020;12:e9837 https://doi.org/10.7759/cureus.9837
3. Eckhert E, Hewitt R, Liedtke M. B-cell maturation antigen directed monoclonal antibody therapies for multiple myeloma. Immunotherapy. 2019;11:801–11. https://doi.org/10.2217/imt-2018-0199
4. Ntanasis-Stathopoulos I, Gavriatopoulou M, Kastritis E, Terpos E, Dimopoulos MA. Multiple myeloma: role of autologous transplantation. Cancer Treat Rev 2020;82:101929 https://doi.org/10.1016/j.ctrv.2019.101929
5. Chim CS, Kumar SK, Orlowski RZ, Cook G, Richardson PG, Gertz MA, et al. Management of relapsed and refractory multiple myeloma: novel agents, antibodies, immunotherapies and beyond. Leukemia 2018;32:252–62. https://doi.org/10.1038/leu.2017.329
6. Butova R, Vychytilova-Faltejskova P, Souckova A, Sevcikova S, Hajek R. Long non-coding RNAs in multiple myeloma. Non-coding RNA. 2019;5:13 https://doi.org/10.3390/ncrna5010013
7. Sanchez Calle A, Kawamura Y, Yamamoto Y, Takeshita F, Ochiya T. Emerging roles of long non-coding RNA in cancer. Cancer Sci. 2018;109:2093–2100. https://doi.org/10.1111/cas.13642
8. Yang Y, Peng XW. The silencing of long non-coding RNA ANRIL suppresses invasion, and promotes apoptosis of retinoblastoma cells through the ATM-E2F1 signaling pathway. Biosci Rep. 2018;38:BSR20180558 https://doi.org/10.1042/BSR20180558
9. Gao Y, Fang P, Li WJ, Zhang J, Wang GP, Jiang DF, et al. LncRNA NEAT1 sponges miR-214 to regulate M2 macrophage polarization by regulation of B7-H3 in multiple myeloma. Mol Immunol. 2020;117:20–28. https://doi.org/10.1016/j.molimm.2019.10.026
10. Chen X, Liu Y, Yang Z, Zhang J, Chen S, Cheng J. LINC01234 promotes multiple myeloma progression by regulating miR-124-3p/GRB2 axis. Am J Transl Res. 2019;11:6600–18
11. David A, Zocchi S, Talbot A, Choisy C, Ohnona A, Lion J, et al. The long non-coding RNA CRNDE regulates growth of multiple myeloma cells via an effect on IL6 signalling. Leukemia. 2020 https://doi.org/10.1038/s41375-020-01034-y
12. Lee YS, Dutta A. MicroRNAs in cancer. Annu Rev Pathol. 2009;4:199–227. https://doi.org/10.1146/annurev.pathol.4.110807.092222
13. Tang XJ, Wang W, Hann SS. Interactions among lncRNAs, miRNAs and mRNA in colorectal cancer. Biochimie 2019;163:58–72. https://doi.org/10.1016/j.biochi.2019.05.010
14. Shen X, Kong S, Yang Q, Yin Q, Cong H, Wang X, et al. PCAT-1 promotes cell growth by sponging miR-129 via MAP3K7/NF-κB pathway in multiple myeloma. J Cell Mol Med. 2020;24:3492–503. https://doi.org/10.1111/jcmm.15035
15. Yang N, Chen J, Zhang H, Wang X, Yao H, Peng Y, et al. LncRNA OIP5-AS1 loss-induced microRNA-410 accumulation regulates cell proliferation and apoptosis by targeting KLF10 via activating PTEN/PI3K/AKT pathway in multiple myeloma. Cell Death Dis 2017;8:e2975 https://doi.org/10.1038/cddis.2017.358
16. Petri A, Dybkær K, Bøgsted M, Thrue CA, Hagedorn PH, Schmitz A, et al. Long noncoding RNA expression during human B-cell development. PLoS ONE. 2015;10:e0138236 https://doi.org/10.1371/journal.pone.0138236
17. Zhang X, Zhang Y, Yang J, Li S, Chen J. Upregulation of miR-582-5p inhibits cell proliferation, cell cycle progression and invasion by targeting Rab27a in human colorectal carcinoma. Cancer Gene Ther. 2015;22:475–80. https://doi.org/10.1038/cgt.2015.44
18. Jin Y, Tao LP, Yao SC, Huang QK, Chen ZF, Sun YJ, et al. MicroRNA-582-5p suppressed gastric cancer cell proliferation via targeting AKT3. Eur Rev Med Pharm Sci. 2017;21:5112–20. https://doi.org/10.26355/eurrev_201711_13827
19. Li J, Gao J, Tian W, Li Y, Zhang J. Long non-coding RNA MALAT1 drives gastric cancer progression by regulating HMGB2 modulating the miR-1297. Cancer Cell Int. 2017;17:44 https://doi.org/10.1186/s12935-017-0408-8
20. Han Q, Xu L, Lin W, Yao X, Jiang M, Zhou R, et al. Long noncoding RNA CRCMSL suppresses tumor invasive and metastasis in colorectal carcinoma through nucleocytoplasmic shuttling of HMGB2. Oncogene. 2019;38:3019–32. https://doi.org/10.1038/s41388-018-0614-4
21. Pu J, Tan C, Shao Z, Wu X, Zhang Y, Xu Z, et al. Long non-coding RNA *PART1* promotes hepatocellular carcinoma progression via targeting miR-590-3p/*HMGB2* axis. Onco Targets Ther. 2020;13:9203–11. https://doi.org/10.2147/OTT.S259962
22. Stros M, Ozaki T, Bacikova A, Kageyama H, Nakagawara A. HMGB1 and HMGB2 cell-specifically down-regulate the p53- and p73-dependent sequence-specific transactivation from the human Bax gene promoter. J Biol Chem. 2002;277:7157–64. https://doi.org/10.1074/jbc.M110233200
23. National Research Council (US) Committee for the Update of the Guide for the Care and Use of Laboratory Animals. Guide for the care and use of laboratory animals. 8th ed. Washington, DC: National Academies Press; 2011. p. 11–104
24. Wang L, Park HJ, Dasari S, Wang S, Kocher JP, Li W. CPAT: Coding-Potential Assessment Tool using an alignment-free logistic regression model. Nucleic Acids Res 2013;41:e74 https://doi.org/10.1093/nar/gkt006
25. Chen H, Li M, Xu N, Ng N, Sanchez E, Soof CM, et al. Serum B-cell maturation antigen (BCMA) reduces binding of anti-BCMA antibody to multiple myeloma cells. Leuk Res. 2019;81:62–66. https://doi.org/10.1016/j.leukres.2019.04.008
26. Liu D, Qiu M, Jiang L, Liu K. Long noncoding RNA HOXB-AS1 is upregulated in endometrial carcinoma and sponged miR-149-3p to upregulate Wnt10b. Technol Cancer Res Treat. 2020;19:1533033820967462 https://doi.org/10.1177/1533033820967462
27. Li QY, Chen L, Hu N, Zhao H. Long non-coding RNA FEZF1-AS1 promotes cell growth in multiple myeloma via miR-610/Akt3 axis. Biomed Pharmacother. 2018;103:1727–32. https://doi.org/10.1016/j.biopha.2018.04.094
28. Handa H, Honma K, Oda T, Kobayashi N, Kuroda Y, Kimura-Masuda K, et al. Long noncoding RNA *PVT1* is regulated by bromodomain protein BRD4 in multiple myeloma and is associated with disease progression. Int J Mol Sci. 2020;21:E7121 https://doi.org/10.3390/ijms21197121
29. Wang Y, Wang H, Ruan J, Zheng W, Yang Z, Pan W. Long non-coding RNA OIP5-AS1 suppresses multiple myeloma progression by sponging miR-27a-3p to activate TSC1 expression. Cancer Cell Int. 2020;20:155 https://doi.org/10.1186/s12935-020-01234-7
30. Pan Y, Zhang Y, Liu W, Huang Y, Shen X, Jing R, et al. LncRNA H19 overexpression induces bortezomib resistance in multiple myeloma by targeting MCL-1 via miR-29b-3p. Cell Death Dis. 2019;10:106 https://doi.org/10.1038/s41419-018-1219-0
31. Yang X, Huang H, Wang X, Liu H, Liu H, Lin Z. Knockdown of lncRNA SNHG16 suppresses multiple myeloma cell proliferation by sponging miR-342-3p. Cancer Cell Int. 2020;20:38 https://doi.org/10.1186/s12935-020-1118-1
32. Li L, Ma L. Upregulation of miR-582-5p regulates cell proliferation and apoptosis by targeting AKT3 in human endometrial carcinoma. Saudi J Biol Sci. 2018;25:965–70. https://doi.org/10.1016/j.sjbs
33. Liu J, Liu S, Deng X, Rao J, Huang K, Xu G, et al. MicroRNA-582-5p suppresses non-small cell lung cancer cells growth and invasion via downregulating NOTCH1. PLoS ONE. 2019;14:e0217652 https://doi.org/10.1371/journal.pone.0217652

34. Wang LL, Zhang M. miR-582-5p is a potential prognostic marker in human non-small cell lung cancer and functions as a tumor suppressor by targeting MAP3K2. Eur Rev Med Pharm Sci. 2018;22:7760–7. https://doi.org/10.26355/eurrev_201811_16397
35. Xu CH, Xiao LM, Liu Y, Chen LK, Zheng SY, Zeng EM, et al. The lncRNA HOXA11-AS promotes glioma cell growth and metastasis by targeting miR-130a-5p/HMGB2. Eur Rev Med Pharm Sci. 2019;23:241–52. https://doi.org/10.26355/eurrev_201901_16770
36. Wu ZB, Cai L, Lin SJ, Xiong ZK, Lu JL, Mao Y, et al. High-mobility group box 2 is associated with prognosis of glioblastoma by promoting cell viability, invasion, and chemotherapeutic resistance. Neuro Oncol 2013;15:1264–75. https://doi.org/10.1093/neuonc/not078
37. Zhang P, Lu Y, Gao S. High-mobility group box 2 promoted proliferation of cervical cancer cells by activating AKT signaling pathway. J Cell Biochem. 2019;120:17345–53. https://doi.org/10.1002/jcb.28998